Click evoked Middle Ear Muscle Reflex: Implications for Medial Olivocochlear System Assays

Sriram Boothalingam[1] and Shawn S. Goodman[2]

[1]Department of Communication Sciences and Disorders
Waisman Center
University of Wisconsin, Madison, WI 53705

[2]Department of Communication Sciences and Disorders
University of Iowa, Iowa City 52252

Abstract
This study describes a time series-based method of middle ear muscle reflex (MEMR) detection using bilateral clicks, with implications for otoacoustic emission (OAE)-based medial olivocochlear reflex (MOCR) assays. Although current click-based methods can detect changes in the OAE evoking stimulus to monitor the MEMR, these methods do not discriminate between true MEMR-mediated vs. artifactual changes in the stimulus. We measured MEMR in 20 young clinically normal hearing individuals using a series of clicks presented at six levels (65 to 95 dB peak-to-peak SPL in 6 dB steps). Results were well-approximated by double-exponential functions. The change in ear canal pressure due to MEMR increased monotonically as a function of click level but non-monotonically with frequency. MEMR thresholds estimated using this method were lower than that obtained from a clinical tympanometer in ~94% of the participants. It is recommended that the OAE-evoking stimulus be monitored to determine the presence of MEMR across a wide band of frequencies in MOCR assays. A time series-based method, along with statistical tests, may provide additional confidence in detecting the MEMR. MEMR effects were smallest at 2 kHz which may provide avenues for minimizing the MEMR influence on the MOCR.

Introduction
Two auditory reflexes exert influence on peripheral auditory signal processing. The middle ear muscle reflex (MEMR) influences signal transfer by altering the impedance characteristics of the middle ear, and the medial olivocochlear reflex (MOCR) inhibits the cochlear active process (review: Guinan, 2006). Animal models suggest both of these processes benefit the organism by protecting cochlear structures from loud sounds and improving signal-to-noise ratio (Liberman & Guinan, 1998). As such, understanding the functioning of these two reflexes in humans holds both scientific and clinical value.

Otoacoustic emissions (OAE)-based assays provide a convenient, non-invasive means to investigate MOCR effects in humans. However, many of the stimuli which activate the MOCR also simultaneously activate the MEMR. Both the input to cochlea (stimulus) and the retrograde emissions can be significantly altered by MEMR activation (Guinan,

Backus, Lilaonitkul, & Aharonson, 2003). Thus, a major impediment to measuring MOCR is that, when active, the MEMR effects on OAEs can masquerade as MOCR effects (Goodman, Mertes, Lewis, & Weissbeck, 2013; Goodman, Venkitakrishnan, Adkins, & Mueldener, 2018; Guinan et al., 2003; Zhao & Dhar, 2009). Therefore, a key to understanding the contributions of the two reflexes is accurate detection and measurement. Here we propose an approach to MEMR detection based on a click stimulus time series analyzed in discrete frequency bands.

There have been multiple efforts among researchers to develop methods capable of detecting MEMR activation during MOCR measurements. Backus and Guinan (2007) introduced a stimulus frequency (SF)OAE phase gradient-based method of MEMR detection. The rationale was that MEMR-mediated changes in the SFOAE delay would be much shorter compared to MOCR-mediated changes. Other researchers have used concurrently presented tones (602 Hz and/or 226 Hz) to monitor the MEMR during SFOAE measurements (Goodman and Keefe, 2006; Zhao & Dhar, 2009). Abdala, Mishra, and Garinis (2013) monitored stimulus changes in their two-tone distortion product (DP)OAE stimulus to detect MEMR activation. The rationale for these latter two methods was that the MEMR activation would alter stimulus reflectance, causing a change in the ear canal stimulus pressure. Based on work by Feeney, Keefe, and Marryott (2003), Abdala et al. (2013) suggested that a stimulus level change of 0.12 dB (1.4%) is indicative of MEMR activation.

More recent investigations have employed transient stimuli such as clicks and tonebursts to detect the MEMR. Boothalingam and Purcell (2015) applied the same approach as Abdala et al. (2013) to clicks and reported no MEMR activations for low-level click/contralateral noise combination (55 dB peSPL/60 dB SPL, respectively). Mertes (2020) established critical differences in click stimulus for detecting MEMR based on group data. Marks and Siegel (2017) monitored tonebursts in a level-series. Goodman and colleagues (Goodman et al., 2013; Mertes and Goodman, 2015) used a resampling-based approach to establishing statistically whether the changes in the stimulus level indicate MEMR activation. Goodman et al. (2018) included stimulus phase in the measurements, noting that while including phase increased the sensitivity of MEMR detections, it was not possible to disentangle the MEMR effects on the MOCR when both reflexes were active. Results from a majority of the above studies corroborate findings by Feeney and Keefe (Feeney et al., 2003; Feeney and Keefe, 2001) that the MEMR is activated at much lower levels (up to 21 dB) than that estimated by clinical instruments. Therefore, it is imperative that establishing the presence/absence of the MEMR in MOCR assays is not assumed based on MEMR thresholds from standard clinical instruments.

Despite the significant improvements made in recent years, uncertainty remains regarding how best to ascertain whether observed changes in OAEs represent purely MOCR-mediated activity or are a combination of both MEMR and MOCR activity. One reason is that MEMR effects are frequency dependent, resulting in increased stimulus reflection at the eardrum at lower frequencies but reduced reflection at higher frequencies (Keefe, Bulen, Arehart, et al., 1993; Feeney and Keefe, 1999; Borg, 1968).

As such, when frequency-specific changes are not considered (e.g., Boothalingam and Purcell, 2015; Mertes, 2020), MEMR detection may be less sensitive. This is because MEMR-induced stimulus changes at the lower and higher frequencies may partially cancel out and falsely reflect little or no change. Such cancellations may be a larger issue for broadband stimuli such as clicks than for DPOAE- or SFOAE-based assays.

Another palpable reason for the uncertainty is that the presence of MEMR in all the aforementioned methods is deduced by comparing the change in stimulus magnitude from only two conditions: with- and without-an acoustic efferent activator (typically contralateral noise). While resampling methods can indicate whether a reliable difference in stimulus level exists between the two conditions, the difference cannot always be attributed to the MEMR. Pressure changes due to probe movement and/or changes in middle ear pressure during recording can also produce stimulus level differences between conditions (Goodman et al., 2013). For this reason, evaluating the time course of pressure changes in the recorded stimulus level may be useful. The MOCR and the MEMR demonstrate an exponential onset and offset (Backus and Guinan, 2006; Hung and Dallos, 1972; Kim, Dorn, Neely, and Gorga, 2001; Liberman, Puria, and Guinan, 1996; Meinke, Stagner, Martin, and Lonsbury-Martin, 2005; Srinivasan, Keil, Stratis, Woodruff-Carr, and Smith, 2012). This predictable behavior can be leveraged to identify true MEMR responses, both visually and statistically.

The purpose of the present study was to address these sources of uncertainty by introducing a method that evaluates pressure recordings of click trains in order to identify the presence of MEMR. The kinetics of the resulting time series are evaluated in a frequency-specific manner. When paired with statistical tests, the approach provides a sensitive, objective method for detecting middle ear pressure changes over time, and allows for discrimination between changes due to MEMR versus other sources.

Method

Participants

Twenty young, clinically-normal hearing volunteers (mean age: 22±2.7 years; 2 males) participated in the study. Clinically normal hearing was established by an unremarkable otoscopy examination, behavioral hearing thresholds ≤20 dB HL between 0.25 and 8 kHz (SmartAud, Intelligent Hearing Systems, FL), type-A tympanograms (Titan, Interacoustics, Denmark), and measurable DPOAEs (0.5-6 kHz; 1/3rd octave intervals; 6 dB signal-to-noise ratio [SNR] criterion) (SmartDPOAE, Intelligent Hearing Systems, FL). Middle-ear muscle reflex thresholds were also measured in all participants using a clinical system (Titan, Interacoustics, Denmark). All participants provided written informed consent prior to participating in the study. Their participation counted towards extra-credit for various courses in the undergraduate program within the Department of Communication Sciences and Disorders. All study procedures were approved by the Health Sciences Institutional Review Board at the University of Wisconsin, Madison.

Experimental set-up

Stimuli were digitally generated in Matlab (Mathworks, MA) using an iMac (Apple, CA). The iMac was interfaced with a sound card (Fireface UFX+, RME, Germany) for analog-to-digital-to-analog conversion at a sampling rate of 96 kHz and delivered stimuli to the participants' ears bilaterally using a dual-probe ER10X system (Etymotic Research, IL). The ER10X probe microphones recorded the ear canal pressure bilaterally. Synchronous playback and recording of signals were done using the Auditory Research Lab Audio Software suite (Goodman, 2017) in Matlab. The ER10X probes were held securely in place in participants' ears by (1) hanging the cables from the sound booth ceiling, (2) attaching them to hollowed-out ear muffs with only the headband and cushion in place (Mpow 035, Mpow, CA), and (3) puttying around the probes in-ear using silicone earmold putty (Silicast, Westone Laboratories, CO). In addition, an in-situ stimulus calibration was done before the start of every measurement condition. The calibration results were monitored throughout the experiment for gross deviations.

All testing was conducted in a double-walled sound-attenuating sound booth where participants sat comfortably in a recliner for the duration of the experiment and watched a silent closed-captioned movie. Participants were asked to sit relaxed, not move, and swallow as few times as comfortable, and not sleep. They were allowed to move and do any noisy activities (e.g., cough) between each experimental condition, i.e., roughly every 10 mins. The entire experiment took about an hour to complete.

Stimulus, calibration, and paradigm

The level of the clicks was varied from 65 dB peak-to-peak (pp) SPL to 95 dB ppSPL in 6 dB steps in 6 separate stimulus level *conditions*. Stimuli were presented bilaterally. Each *block* consisted of a 1.008 s long click train, (henceforth referred nominally as 1 s) and a 0.742 s silent period. Each block was repeated 335 times per stimulus level condition. The click train consisted of 63 clicks presented at a rate of 62.5 clicks per second. This click rate translated to an *epoch* size of 16 ms. Unlike a traditional contralateral noise elicitor paradigm, we used the CEOAE-evoking clicks to also elicit the MEMR. The 62.5 Hz rate elicits robust MOCR at 80 dB ppSPL (Boothalingam et al., 2018), and the 1 s long click train was expected to allow the MEMR to reach steady state (Hung and Dallos, 1972).

Click stimuli were generated in the frequency domain. Click spectra were bandlimited between 0.8 and 6 kHz and flattened at the eardrum using forward pressure level (FPL) calibration, in order to homogenize cochlear stimulation across participants by accounting for the differences in external and middle ear impedance characteristics. Detailed descriptions of FPL calibration can be found other reports (e.g., Scheperle, Neely, Kopun and Gorga, 2008; Souza, Dhar, Neely, and Siegel, 2014; Dewey and Dhar, 2017). Briefly, prior to data collection, Thevenin-equivalent source calibration of the probes were obtained for known acoustic loads of tube lengths 2.9, 3.6, 4.15, 5.2, 6.9 cm (diameter = 8 mm). The different lengths of the tube were achieved by moving the piston in the inbuilt calibration cavity of the ER10X system. The load (participants' ear) calibration was performed before each condition, i.e., roughly every 10 mins, to obtain the ear canal and middle ear impedance, surge impedance, and the pressure

reflectance. These estimates were used to calculate the forward and reverse pressures in the ear canal and build the external and middle ear transfer function (Rasetshwane and Neely, 2011). Based on the transfer function between 0.8 and 6 kHz, correction factors were created to generate a flat spectrum click at the eardrum. This matrix was then inverse Fourier transformed to the time domain. Clicks were then scaled to obtained the desired in-ear ppSPL level.

Pilot work suggested that in some participants, it was not possible to achieve the desired level at the highest click level condition (95 dB ppSPL) due to loudspeaker output limitations. To avoid this issue and reduce loudspeaker ringing, all the aforementioned calibration procedures, including source calibration, were done for clicks simultaneously presented through the two loudspeakers of each probe, and this allowed the highest click level to be reached. The duration of the final acoustic click and its ringing in an ear simulator was roughly 3.5 ms.

Response analysis

Recorded ear canal pressure was first bandpass filtered between 0.7 and 6 kHz. Although the click stimulus bandwidth extended to 6 kHz, preliminary data analysis and prior studies have suggested minimal MOCR activations past 3.5 kHz (Goodman et al., 2013). Therefore, the click stimuli were also considered only between 0.89 to 3.5 kHz in the analyses reported below. After filtering, post-hoc artifact rejection was applied. Epochs with root-mean-squared (RMS) amplitude >2.25 times the interquartile range were discarded as artifacts (Goodman, Fitzpatrick, Ellison, Jesteadt, and Keefe, 2009). The rejection rate by this method was approximately 10% of recordings, across participants.

Stimulus extraction

Stimulus level was estimated from ear canal pressure waveforms that were time windowed between -1 and 3.5 ms, with time zero defined as the location of the maximum excursion of the click pressure waveform. Raised cosine onset and offset ramps (0.5 ms duration) were applied to the windowed pressures. Together with the restricted frequency range of 0.89-3.5 kHz, this short window length was expected to avoid contamination from OAEs in the stimulus window. OAE contamination could be a problem because MOCR-mediated changes in the OAE could masquerade as MEMR activity. Given the dispersion in OAE frequency-latency relationship of reflection-generated emissions (e.g. SFOAEs and CEOAEs), it is highly unlikely that emissions below 3.5 kHz would be included in the stimulus window (<3.5 ms; Shera, Guinan, and Oxenham, 2002). Even if some emission pressure is included in the stimulus window by way of accounting for the higher stimulus levels, at these high levels the emission to stimulus pressure ratio is highly skewed towards the stimulus pressure. At high levels, the addition of the emission pressure likely adds an insignificant amount to the stimulus, and as such the change due to the MOCR is also unlikely to be significant enough to influence the MEMR measurements (Keefe, Fitzpatrick, Liu, Sanford, and Gorga, 2010).

Waveforms within this time window were converted from SPL to forward pressure level (FPL) and reverse pressure level (RPL) using the source and load impedances obtained

during stimulus calibration (Rasetshwane and Neely, 2011; Scheperle et al., 2008). Preliminary analyses (not shown) suggested no difference in the MEMR estimated using the three types of pressure waveforms. We chose to use RPL in all further analyses. Noise floor levels were estimated as the standard error of mean (SEM; Goodman et al., 2009) of the 335 spectra at each point on the time series.

Spontaneous and synchronized spontaneous (S/SSOAEs) pose challenges similar to the CEOAEs in MEMR estimation by including MOCR effects. To rule out MOCR contamination of the MEMR, we measured and removed S/SSOAEs. The last click epoch was used to monitor SSOAEs in a temporal window extending from 20-40 ms after the click. This time window was transformed via FFT, and SSOAEs were identified as spectral peaks $\geq$10 dB above the noise-floor and were greater than -12 dB SPL (similar to Marshall, Miller, Guinan, et al., 2014). Frequencies where S/SSOAEs were present were applied a weighting of zero in the energy weighted averaging processes within each frequency bin (explained further below). As such, S/SSOAEs likely have no bearing on MEMR estimation.

MEMR estimation

MEMR magnitude was estimated by examining the RPL of the stimulus time series. The recorded waveforms across the time series were arranged into a matrix, X, with i = 336 rows (3.5 ms duration x 96 kHz sampling rate) and j = 63 columns (epochs). Each column in X was the mean waveform across 335 repetitions at the jth point in the time series. Each of these waveforms was Fast Fourier transformed and the absolute magnitude at each point in the time series was expressed relative to the magnitude of the first point. This metric of relative change, Δ, was reduced from the full set of Fourier coefficients to third-octave bands by taking the energy weighted average of the subset of elements in Δ corresponding to the passband frequencies of a bank of third-octave filters with center frequencies 1, 1.3, 1.6, 2, 2.5, and 3.2 kHz. This value was then expressed in dB.

At each of the six frequency bands, the dB values across 63 time-points provided an estimate of the change in the stimulus magnitude over the course of 1 s. No change in the stimulus corresponded to a value of 0 dB, while positive or negative values were interpreted as an increase or decrease in the stimulus magnitude relative to the magnitude at the first time-point. The MEMR time series from one participant representing typical time series behavior and one representing atypical behavior is shown in Fig. 1. About 20% (4 out of 20) showed similar atypical behavior at different frequency bands. The magnitude and time-constants of the MEMR were estimated from the time series using a physiologically-motivated double-exponential model fit to the data (Liberman et al., 1996; Kim et al., 2001; Meinke et al., 2005; Backus and Guinan, 2006; Srinivasan et al., 2012), i.e., fit lines in Fig. 1 (top panels):

$$f(t) = C + m_f * \exp\left(-\frac{t}{\tau_f}\right) + m_s * \exp\left(-\frac{t}{\tau_s}\right), \qquad \text{(Eq. 1)}$$

where, $f(t)$ is the fit as a function of time (t). The variables m_f and m_s are the magnitudes of the fast and slow components of the fits, respectively. The variables τ_f and τ_s are the fast and slow time-constants, respectively. C is the constant term representing the offset along the y-axis. Because we fit lines to normalized data (Δ), this term is zero. Considering our time-course measurement terminated at 1 s, it was not possible to reliably estimate the slow time-constants from our data. As such, only the time-constant of the first, short component, hereafter referred to as $\mathbf{MEM}_{\boldsymbol{\tau}}$, is reported. This time constant corroborates the time-constants reported previously for the MEMR (Hung and Dallos, 1972). The two components are, however, necessary because a single exponential does not model the data as accurately as a double exponential. The estimate of MEMR magnitude change, hereafter referred to as **MEM**, was the final value (at time 1 s) of the fitted function. This value represented the magnitude of change after 1 second, relative to the starting value.

Comparison with a clinical instrument

MEMR elicited with broadband noise in a clinical instrument (Titan, Interacoustics, Denmark) was also measured for purposes of comparison with the MEMR threshold estimated using the proposed method. While not the focus of the study, this comparison allowed for corroboration of lower thresholds in click-based wideband MEMR estimation relative to clinical instruments reported by others (e.g., Feeney and Keefe, 2001; Feeney et al., 2003; Marks and Siegel, 2017). In the present study, MEMR threshold from the time series data was calculated as the lowest level at which at least one of the six frequency bands showed significant MEMR activity (explained below). Threshold from the clinical tympanometer was calculated as the lowest level at which the activator (broadband noise) caused a 0.02 ml change in admittance.

False positive check

To ensure the changes in stimulus levels were unrelated to system artifacts or other non-physiological factors, we ran all conditions of the experiment in an ear simulator (Type 4137; Bruel & Kjaer, Naerum, Denmark). The outputs from the analysis of this data for the 1 kHz band across levels are plotted in the lower panel of Fig. 1. There was no evidence of any systematic changes in the stimulus estimate across time and level. No line fits are shown because none of the fits were significant (explained below). Compared to normal hearing participants, the range of random stimulus changes in the ear simulator was 2-3 orders of magnitude smaller. We also did not find any frequency effects (data not shown for ease of visualization). This check provides confidence that any changes in the stimulus that we observe must have physiological origins and were not system-related.

[Fig. 1 about here]

Statistical tests

MEMR activity was deemed present in individuals if the exponential fits were significant in the Heller-Heller-Gorfine test (HHG; Heller, Heller, and Gorfine, 2013). The HHG is a

nonparametric test of association between two random vectors. It is implemented between two random vectors of the same dimensions and is sensitive to nearly any form of dependence. We implemented the test by letting the first vector be an MEMR time series sequence. The comparison vector was the double-exponential fit to that same sequence. Implemented in this manner, we tested the null hypothesis that there was no association between the two vectors, i.e. that both vectors were random sequences. Since the vector representing the exponential fit was never a random sequence, we were in effect testing whether the MEMR time series was a random vector. If the MEMR time series was not random (i.e. if there was any systematic change across time), then the HHG test detected a dependence between the two vectors, the null hypothesis was rejected, and that time series was considered to show evidence of either MEMR, some other systematic change over time, or both. Significance of the comparison (*p*-value) was obtained by generating confidence intervals from bootstrapping the HHG test 1000 times. Because each participant had data at six frequencies at each of the six stimulus levels, *p*-values were corrected for alpha inflation using the False Discovery Rate (FDR; Benjamini and Hochberg, 1995) method.

To study MEM and MEM_τ group data, a linear mixed-effects model (*lme4* package in R; Bates, Mächler, Bolker, and Walker, 2015; R Core Team, 2014) was fit to dependent variables MEM and MEM_τ with fixed-effects of predictors level (L), frequency (f), and the interaction between level and frequency and random-effects of participants and random slopes for level. Stimulus level was treated as a continuous variable because levels were incremented in discrete steps and frequency was treated as a categorical variable because Δ was discretized by averaging in 1/3rd octave bands:

$$MEM\ (or)\ MEM_\tau = \beta_0(1\ kHz) + \beta_1 f + \beta_2 L + \beta_3 f * L + b_i, \qquad (Eq.2)$$

β_0 is the intercept when level is at the origin and frequency is 1 kHz, β_1 for each of the five frequencies (1.2, 1.6, 2, 2.5, and 3.2 kHz) is the simple effect, i.e., the intercept, of frequency when the level at origin with 1 kHz as the reference condition because frequency is treated as a categorical variable, β_2 is the slope of the level, β_3 is the interaction of level and frequency, i.e., the difference in the simple slopes of level for the six frequencies, and b_i is the random-effects intercept for each participant i. The model was tested for significance using analysis of variance (ANOVA).

To study MEMR detections in the form of percentage detections (%detection = *n* participants with significant MEM/group size) a general linear mixed-effects model was fit to the dependent variable %detection in a fashion similar to the linear mixed-effects model for MEM and MEM_τ (Eq 4), except logistic regression was used instead of linear regression as the data were binominal (MEMR present vs. absent as determined by the HHG test) with the link option as logit.

Results

Stimulus change in the time series shows frequency-specific changes in middle ear impedance

The increase in stiffness in the middle ear due to the MEMR action will generally attenuate low frequency energy from reaching the cochlea more than high frequency energy. However, this relationship is non-monotonic. Data from Feeney and Keefe (1999; 2001) on the change in wideband reflectance due to MEMR activation show a reversal, i.e., reduced reflectance, or increased absorbance, between 1 and 1.5 kHz. Based on these prior data, we expected a reduction in the recorded ear canal stimulus level for the lower third-octave bands (1-1.6 kHz) and a relative increase in the recorded ear canal stimulus level for frequency bands ≥1.6 kHz. The time series for the six third-octave bands for each stimulus level, averaged across participants, is shown in Fig. 2. The time series of the MEMR at different frequencies was consistent with these expectations. The transition in the direction of change between the low vs. high frequencies appears to occur between 1.6 and 2 kHz corroborating prior reports (Feeney and Keefe, 1999; 2001; Schairer et al., 2007). An unexpected observation in the time series is that lower frequencies (1 and 1.2 kHz) appear to approach steady-state gradually close to 1 s, but the higher frequencies reverse course towards baseline shortly after onset, i.e., adapt to the presence of the stimulus.

The distribution of MEM across individuals is shown by the box plots in Fig. 3. MEM fits that did not pass the inclusion criteria (HHG test) were excluded from these plots. The number of subjects at each level and frequency combination (*n*-sizes) are the same as those given in Fig. 2. Level and frequency effects are apparent: MEM clusters around zero at lower levels and demonstrates a larger spread as level increases.

[Fig. 2 about here]

[Fig. 3 about here]

MEMR magnitude increases with level and decreases with frequency

In general, the data suggest that the Δ is larger at lower (<2 kHz) relative to higher frequencies (>2 kHz) at all stimulus levels. As seen in Fig. 4, the time series grew monotonically with increasing level at all frequencies. However, at higher frequencies (≥2 kHz), the time series tended to return to the baseline more strongly at the highest level. Note that these time series are averaged across participants where the time series for the same frequency can in some instances go in opposite directions (e.g., Fig 2 Atypical panel). The true magnitude of the MEMR can be compared across levels and frequencies when the absolute values (|MEM|) are plotted as input-output (IO) plots. In Fig. 5 IO for each frequency is plotted first in a separate panel and then summarized together in the top right panel (MEM-IO panel).

[Fig. 4 about here]

Growth of |MEM| was best approximated by a single exponential function. When the mean fits (thick lines) are viewed together (Fig. 5 MEM-IO panel) the differences in MEM growth with level as a function of frequency is apparent: lower frequencies undergo larger changes than higher frequencies. When the data are visualized as a function of frequency (Fig. 5 bottom right panel, MEM-Tx) with separate lines for each level, a MEM transfer function emerges. MEM grows non-monotonically with frequency and displays an asymmetric U-shape with the minima around 2 kHz, most prominent at 95 dB ppSPL.

[Fig. 5 about here]

To study the data inferentially, a linear mixed-effects model was used (see Statistical Tests section). Only levels 77 through 95 dB ppSPL were included in the model as the lower levels had few MEMR activations. Given the exponential relationship between MEM and stimulus level, the values of MEM were linearized (by taking the logarithm of the absolute value) prior to fitting with a mixed-effects model. This transformation was necessary because linear models assume a linear relationship between the dependent and the predictor variables. Finally, to make the model estimates easier to interpret, we moved the origin of the predictor (level) to 77 dB ppSPL by subtracting the lowest stimulus level (77 dB ppSPL) from all levels. We first compared two models: with and without the level by frequency interaction term Eq (2). The interaction term was not significant (p=0.63) and was subsequently dropped from the model. The summary of results of the model without the interaction term is tabulated in Table 1.

[Table 1 about here]

The lack of significant frequency by level interaction suggests that despite the difference in the magnitude of MEMR change with level at each frequency, the rate of change of magnitude with level is not different across frequencies, at least between 77 and 95 dB ppSPL. That is, the fit lines in Fig. 5 MEM-IO (top right) panel are different in their intercepts but not slopes (note that the exponential slopes were linearized by taking the logarithm of |MEM|).

The mixed-effects model analysis were followed by pairwise comparisons, corrected for multiple tests using FDR. With the exception of three comparisons, 1.6 vs. 2.5 (p=0.2), 1.6 vs. 3.2 (p=0.8) and 2.5 vs. 3.2 kHz (p=0.3), all other paired comparisons were significant (p<0.046) with most comparisons significant at p<0.001. These comparisons suggest that MEMR magnitudes at different frequencies (statistically modeled as the intercepts) were significantly different from each other, except the aforementioned three frequency pairs.

MEMR kinetics are unaffected by level and frequency

The distributions of the measure of kinetics, MEM_{τ}, are plotted as box plots in Fig. 6. There are fewer data points for MEM_{τ} (re: MEM) because instances where the fast time constant (m_f) was at the bound set based on prior data (500 ms) were not included. This may mean that either the Δ evolved slower than expected or it was noisy for reliable estimation of MEM_{τ}. Similar to MEM (Fig. 3), only the levels 77 through 95 dB ppSPL were included in the linear mixed-effects model fit to the MEM_{τ} data. The summary of this model is presented in Table 2.

[Table 2 about here]

Unlike MEM, neither the main effects nor the interaction was significant for MEM_{τ}, suggesting that the level and frequency do not influence MEM_{τ}. Alternatively, it is possible that (1) the power of our model is inadequate to discern differences in τ given the smaller final sample size for MEM_{τ} or (2) the MEM_{τ} estimates are noisier than the MEM estimates.

[Fig. 6 about here]

MEMR detections increase with level

As shown in Fig. 7, and given the effect of level on MEM, it is not surprising that the number of participants identified as having significant MEMR activity in the group (%detections) increased for all frequencies with increasing level (Fig. 7, bottom panel). This trend was best approximated by logistic fits with stimulus level as the predictor. All fits in this panel were significant ($p<0.001$).

To analyze the %detections inferentially, we fitted data with the general linear mixed-effects logistic model (see Statistical Tests). Like the MEM mixed-effects model, the frequency by level interaction was not significant ($p=0.16$) and was subsequently dropped from the model. This new model results suggested that the level was a significant predictor of %detections (β_2; χ^2 (1, N=20) = 127.1, $p<0.001$) but frequency was not (β_1; χ^2 (5, N=20) = 3.2, $p=0.7$). This result is consistent with the logistic fit-lines in the 'Fits' (bottom right) panel of Fig. 7. These results suggest that, unlike MEM, %detections do not vary by frequency. By cautiously extrapolating these results to the population, it can be hypothesized that 95% of young normal-hearing individuals will show MEMR activation between 80 and 90 dB ppSPL at all frequencies (vertical dashed lines in Fig. 7 'Fits' panel) when elicited using the stimulus and method proposed in this study.

[Fig. 7 about here]

Comparison with clinical instrument

The MEMR thresholds obtained using the clinical instrument compared to those obtained using the study method are presented as a scatter plot in Fig. 8. Note that clinical MEMR threshold could not be obtained in one participant (technical issue) and in two participants the thresholds were higher than 95 dB SPL, the highest level tested. In the latter two instances, thresholds are shown as 100 dB SPL (open circles). Corroborating prior studies, the study method showed lower thresholds for all but one participant. The mean difference between the clinical method and the study method was 12.35 (SD = 7.15) dB, with the largest difference being 24 dB and the smallest difference -1 dB, where the negative sign indicates the study method produced higher threshold. This result should be viewed cautiously due to differences in the stimulus type, level, mode of presentation (contralateral in clinical vs. bilateral in the study), atmospheric vs. tympanic peak pressure, and different criteria for defining a threshold in the study vs. clinical instrument.

[Fig. 8 about here]

Discussion

The goal of this study was to describe a time series-based method of MEMR detection using a click train, with implications for OAE-based MOCR assays. Overall, our results showed that the click trains alone do elicit the MEMR and tracking the time series to detect MEMR is a viable method that may be used alongside MOCR assays which use the same click train stimuli. Based on the agreement with frequency-specific changes in the MEMR (i.e., direction of change) reported from wideband estimates, the observed time series are consistent with increased stiffness in the middle ear system due to MEMR activation (Schairer et al., 2007; Feeney and Keefe, 1999; 2001).

MEM frequency effect is consistent with middle ear impedance changes due to increased stiffness

Given the direct relationship between resonant frequency (f) and stiffness reactance (X_s) of a simple harmonic oscillator with a single stiffness and mass reactance ($f \propto X_s$), one would expect that stiffening the ossicular chain via MEMR activation would increase reflectance at the low frequencies and reduce reflectance at the higher frequencies. However, because the middle ear is a complex system with more than one mass and stiffness element, the relationship between impedance and frequency is non-monotonic. Specifically, Feeney and Keefe (1999), and subsequently further studies by Keefe, Feeney, and colleagues (Feeney and Keefe, 2001; Feeney et al., 2003; Schairer et al., 2007; Keefe et al., 2010) reported a prominent notch in the middle ear reflectance between 1 and 1.5 kHz, followed by a relative increase in reflectance beyond 2 kHz. The frequency effects observed in our data are consistent with the frequency-specific

changes reported by Keefe and colleagues for MEMR-mediated changes in their click and chirp probes. When the frequency differences in admittance vs. reflectance are considered (see Fig. 6 of Feeney and Keefe, 1999) our results are also consistent with the results of Bennett and Weatherby (1979). As such, the stimulus changes observed in the time series in our data are consistent with the impedance changes engendered by MEMR activity.

MEM frequency minimum matches impedance zero-crossing

In addition to the similarity in the general frequency effects observed between current data and prior work, the transition, or the zero-crossing, from decreasing to increasing reflectance between 1.6 and 2 kHz matches closely with Keefe, Feeney, and colleagues' work. The asymmetric U-shape in the transfer function (MEM-Tx panel in Fig. 5) illustrates this specific corroboration where the lowest values of MEM in the function are for the 2 kHz band. This 2 kHz transition frequency is observable in all of the wideband MEMR investigations for reflectance (e.g., Feeney and Keefe, 2001), admittance (e.g., Schairer, et al., 2007) and absorbed power level (Feeney et al., 2017). Based on the data of Keefe, Bulen, Arehart, and Burns, 1993, Feeney and Keefe (1999) argued that this null in impedance is due to the middle ear impedance being close to the characteristic impedance of the ear canal. As discussed below (see: Implications for MOCR assays), this null could be of particular importance for MOCR assays.

MEM adaptation is frequency-specific

An important observation in the current study was the difference in the shape of the time series between low and high frequencies (Fig. 4). With the exception of 1.6 kHz, it appears that the lower frequencies reach steady-state on average between 200 and 250 ms and continue to stay in steady-state at the end of the 1 second block. However, the time series of frequencies 2 kHz and above tend to return towards baseline, adapting to the presence of the stimulus. This behavior may at first appear similar to the well-documented MEMR adaptation (for a review, see Wilson, Shanks, and Lily, 1984). However, this differential adaptation across frequencies is from the MEMR monitored with a single low frequency probe (220 or 226 Hz) elicited by low- and high-frequency tonal elicitors. In our data, frequency-specific adaptation is seen in the wideband probe elicited by a wideband elicitor (click). Given that our probe is also the elicitor, the locus of this frequency-specific adaptation cannot be delineated into peripheral vs. central factors. However, there is abundant evidence that point towards a neural and/or central origin for frequency specific adaptation with tonal elicitors (Lutman and Martin, 1978; Mukerji, Windsor, and Lee, 2010; Wilson, Steckler, Jones, and Margolis, 1978). For example, the reflex decay test, which tracks MEMR adaptation, is commonly used in audiology clinics to delineate cochlear vs. retrocochlear pathologies, with faster adaptation for low frequency tonal elicitors taken as indications of auditory nerve or brainstem pathologies (Margolis and Levine, 1991; Stach, 1987; Wilson et al., 1984). We speculate that the adaptation seen in our data results from relaxation of some middle ear structure(s) (e.g., the stapedius muscle, tympanic membrane) over time resulting in a frequency specific change in impedance.

Idiosyncrasies in MEM time series likely reflect stapedius muscle behavior
Similar to the individual data shown in Fig. 1 (Atypical panel), three other participants displayed atypical MEM time series, albeit with much slower transition from negative to positive (or vice versa) change in the time series. The rapid alteration in direction of change (Fig. 1 Atypical panel) has been reported previously by Hung and Dallos (1972). These authors attributed such rapid transition in the direction of change to the stapedius muscle momentarily relaxing before contracting, in a phenomenon referred to as "latency relaxation". Data from Hung and Dallos (1972) on the latency of this change in impedance are similar to the 100-150 ms seen in the present study. Without monitoring the MEMR time series, such idiosyncrasies will go unnoticed while producing puzzling and unexpected changes in reflectance or impedance. Therefore, there is value to monitoring the time course of the reflex in addition to estimating the final magnitude, in order to garner a better understanding of the underlying physiology.

MEM and %detections increase with stimulus level
The MEMR estimate, MEM, was expected to grow with increasing level. This growth function, as seen in Figs. 5 and 6, is monotonic across all frequencies and is best described by a single exponential function. One reason for exponential growth could be that the spectral levels (level per cycle) of the stimulus at the lower levels are at or below the activation threshold of the low-spontaneous-rate (LSR) fibers in many individuals. LSR fibers are thought to belong to the auditory neurons that predominantly innervate a yet-to-be-identified interneuron in the cochlear nucleus which in turn innervate the facial motor neuron (FMN; Kobler, Guinan, Vacher, and Norris, 1992). Axons of the FMN converge on the stapedius muscle to initiate contraction (Guinan, Joseph, and Norris, 1989; Lee, de Venecia, Guinan, and Brown, 2006). When the LSR fibers are stimulated more robustly at progressively higher levels, a rapid increase in the reflex magnitude would be expected. The exponential growth could be related to the steeper slopes of the LSR rate-level function prior to saturation at very high input levels. The differences in rate-level function of the LSR fibers may also have some bearing on the differences in MEM across frequencies (Cooper and Yates, 1994; Liberman, 1978). Such growth in the MEMR function, underlined by the growth in LSR neural function, has been posited to be useful in the diagnosis of subtle and early neural loss such as cochlear synaptopathy (Valero, Hancock, Maison, and Liberman, 2018).

If MEMR-mediated reflectance changes come about due to a single muscle stiffening the ossicular chain, it would be expected that all the frequencies would be similarly affected. The lack of frequency by level interaction in our results align with this notion. However, this all-or-none frequency effect does not seem to apply for the time series, since the high frequencies were observed returning towards baseline at 1 second but the low frequencies were not. While these two results may seem at odds at first, they need not be. This is because, despite the difference in the behavior of the time course across frequency, with increasing level, the magnitude, MEM, nonetheless increases irrespective of the frequency.

A frequency effect was not observed for %detections, that is, all frequencies had similar intercepts and slopes for %detection. Although at the outset it may seem inconsistent

with the significant pairwise difference for almost all frequencies for MEM, detection rate and magnitude of change need not be highly correlated. So long as there is a significant change in the reflectance, i.e., the change is above the reflex threshold with sufficient SNR, the actual magnitude of this reflectance change should not affect detection any further. In other words, above the reflex threshold it is the SNR that is critical for detection, not the magnitude. This result suggests that despite the small MEM at higher frequencies, the reflex nonetheless exists and engenders a small but statistically significant change in the middle ear transfer function. It should, however, be emphasized that statistical significance does not necessarily imply clinical significance. Despite the reflex being present, its functional and clinical consequence may vary with magnitude. These aspects, again, have implications for MOCR assays aiming to avoid MEMR influence.

MEM time-constants are relatively unaffected by level and frequency

The time series in the present paradigm did allow us to deduce time constants from the double-exponential fit. These time constants did not systematically vary as a function of frequency or level but appear to align with the literature. The mean fast time constant (across frequencies and levels) in the study was 199 (SD = 129) ms. This appears to be consistent with latencies reported by prior studies that range between 10 and 200 ms (Jerger and Hayes, 1983; Neergaard and Rasmussen, 1966; Perlman and Case, 1939; Stach, 1987) to up to 400 ms (Dallos, 1964). However, the non-monotonicity in time series at higher frequencies add complication to the interpretation. This illustrates the complexities in monitoring the MEMR with higher frequency probes as discussed earlier. More than the time constants or latencies, the advantage of monitoring the time series, nevertheless, lies in its ability to suggest whether an observed change in the stimulus level is MEMR-mediated or not (explained further in 'Implications for MOCR assays').

Implications for MOCR assays

One of the main goals of this study was to introduce a time series-based method of MEMR detection, which could also be used to minimize MEMR influence on MOCR assays. Our findings suggest that the MEMR is likely to be activated when using click trains which also activate the MOCR. This finding is consistent with previous studies for both the MEMR (Feeney and Keefe, 1999; 2001) and the MOCR (Guinan et al., 2003; Zhao and Dhar, 2012; Abdala et al., 2010; Goodman et al., 2013; Boothalingam and Purcell, 2015; Boothalingam et al., 2018) and as such, provides confidence in our methods. Perhaps the major contribution of the present study comes from its use of a time series. Although there are several methods already available that can detect the presence of a change in the stimulus level between two conditions (e.g., resampling techniques), uncertainty as to whether the observed stimulus change is truly due to MEMR still persistent in these methods. This is because, while a statistically significant change in stimulus level can occur due to the MEMR, it can also occur due to probe slippage, change in middle ear pressure during the course of the experiment, and other physiological/non-physiological factors. Conventional methods that reduce data to only two conditions (with and without noise activator) cannot readily differentiate MEMR-from non-MEMR-mediated change in the stimulus. However, the combination of

significant change in stimulus level and the characteristic exponential change in stimulus level can be used to more certainly attribute the change to the MEMR. Knowing whether the observed stimulus change is due to MEMR can be critical to the decision making on MOCR measurements. For example, if a change is due to MEMR, the stimulus level may need to be lowered. In contrast, if the change is due to other factors, these may need to be addressed followed by a retest.

Monitoring the stimulus to detect MEMR activation is complicated by the reactive component of impedance varying as a function of frequency. Our findings corroborate power reflectance data of Feeney and Keefe (1999; 2001), in that, at lower frequencies (between 0.9 and 2 kHz), the impedance changes due to MEMR activation causes a reduction in stimulus level in the ear canal. In contrast, for frequencies between 2 and 3.2 kHz, the MEMR causes a relative increase in stimulus level in the ear canal. This frequency specific effect means that simple averaging across frequency of the stimulus waveform may underestimate the change in stimulus level due to MEMR activation as opposing direction of changes across frequencies may partially cancel out. Therefore, it is imperative that the stimulus be separated into frequency bands and examined for MEMR-mediated changes in a frequency specific manner.

In a simple comparison in our study (Fig. 8), ~94% of our participants had higher MEMR thresholds when estimated using a clinical tympanometer. This discrepancy is despite the fact that broadband noise was used to elicit the MEMR in the clinical tympanometer, a superior MEMR elicitor relative to clicks (Guinan et al., 2003; Popelka, Karlovich, and Wiley, 1974). Alternatively, it is possible that our bilateral click presentation was more potent in activating the MEMR relative to the contralateral broadband noise. These differences cannot be reconciled when a different instrument and/or MEMR elicitor is used to estimate the MEMR and the MOCR. Therefore, for OAE-based assays of the MOCR, it is critical that the presence of the MEMR is *not* based on MEMR thresholds obtained from clinical tympanometers. We emphasize that monitoring the OAE-evoking stimulus is currently the optimal solution to sensitive monitoring of MEMR activation, in keeping with previous recommendations (Guinan, 2010; Zhao and Dhar, 2012; Mertes and Goodman, 2015; Boothalingam and Purcell, 2015).

Along with a reliable MEMR detection method, already available methods can be used to minimize the probability of evoking it. Very slow click rates (e.g. 5 Hz), low click levels, and a low contralateral noise elicitor level can be used. By allowing enough time for the MEMR to return to baseline the clicks themselves activating the MEMR can be avoided, even if high click levels are used (Goodman et al., *under review*). In addition, estimating the MOCR at multiple elicitor levels will allow room for ignoring levels with MEMR contamination. However, when low click rates/levels or low elicitor levels cannot be used the frequency-specific stimulus changes potentially provide a silver lining for MOCR assays. Our data, along with the data of Feeney and Keefe (1999; 2001), shows that the ear canal and the middle ear impedance has a magnitude zero-crossing between 1.6 and 2 kHz [see Fig. 5 panels MEM-IO and MEM-Tx]. This zero-crossing, or the transition from a reduction in stimulus level to an increment, appears to be consistent in all the 20 participants in our study. It is possible that measuring MOCR

magnitude changes in the 1.6 and 2 kHz region could minimize contamination by the MEMR. An individualized approach to identifying the zero-crossing frequency and capitalizing MOCR measurements close to this frequency has been reported (Goodman et al., 2018). This approach, however, assumes that the presence of MEMR at frequencies outside of the 1.6 to 2 kHz region has minimal influence on the MOCR estimated between 1.6 and 2 kHz. This assumption may not be valid. Although MOC neurons themselves are frequency specific, their dendrites within the cochlea branch extensively (Brown, 2014). Given this branching of the MOC fibers, the MOC inhibition of OAEs between 1.6 and 2 kHz is likely to be affected by inputs to the MOC neurons from other frequency regions. Testing this approach empirically in a future study with two groups of individuals, with and without MEMR, will provide evidence for MEMR influence on the MOCR in this zero-crossing frequency region.

Another possible avenue to minimize MEMR influence is to exploit the faster adaptation of the MEMR at higher frequencies by focusing on MOCR measurements at higher probe frequencies. Again, the same caveats that apply to frequency effects above also apply here. In addition, considering our time course only extended up to ~1 s, it cannot be ascertained whether the adaptation was complete, if it only reached a threshold and continued to exist, or if it crossed the zero-magnitude line and continued to increase in the other direction. Further studies with longer click trains are required to clarify this. It is evident that when the MEMR is detected in an MOCR assay it cannot be teased apart, at least using current methods. Prevention is better than cure applies to MEMR activation in MOCR assays.

Conclusion

We used bilateral click trains to generate time series data, such that MEMR-mediated changes in the impedance characteristics of the middle ear could be tracked both in frequency and time. Our approach allows for (1) the possibility of bilateral activation, (2) presentation of the probe without a separate elicitor, (3) wideband stimulus reflectance monitoring, and (4) verification if that the stimulus change is caused by MEMR by tracking the stimulus-change time series. Our data, like several previous studies, suggest that the MEMR is activated at levels lower than that reported in a clinical tympanometers. As such, MOCR studies that rely on clinical MEMR thresholds to infer the absence of the MEMR must be interpreted with caution. Based on current evidence, monitoring the OAE-evoking stimulus in a frequency specific manner for MEMR activation is the optimal way to detect the possible influence of the MEMR in MOCR assays. The frequency specific changes observed in middle ear impedance may suggest avenues for circumventing or minimizing the effects of the MEMR on MOCR assays but needs further investigation.

Acknowledgements

The authors thank Kristina Broyles for collecting data and Dr. Viji Easwar for help with statistics. This study was supported by funds from the Office of the Vice Chancellor for Research and Graduate Education, University of Wisconsin, Madison to SB.

Tables

Table 1. Summary of linear mixed-effects model and ANOVA with the dependent variable, MEM, and predictors, frequency, level (77-95 dB ppSPL), df = degrees of freedom. The estimates for the frequency are MEM (intercept) at 77 dB ppSPL. The estimate for the level, however, is its effect on MEM averaged across frequencies (slope).

Mixed-effects model results					ANOVA	
Fixed effect	Estimates	Standard error	T-value	*p-value*	*F*-statistic [df]	*p*-value
Intercept ($\beta_{0\text{-}1kHz}$)	-3.2	0.19	-17	<0.001	26.7 [5,366]	<0.001
Frequency ($\beta_{1\text{-}1.3\ kHz}$)	-0.4	0.18	-2.1	0.036		
Frequency ($\beta_{1\text{-}1.6\ kHz}$)	-0.99	0.18	-5.5	<0.001		
Frequency ($\beta_{1\text{-}2\ kHz}$)	-1.9	0.18	-10.3	<0.001		
Frequency ($\beta_{1\text{-}2.5\ kHz}$)	-1.2	0.18	-6.8	<0.001		
Frequency ($\beta_{1\text{-}3.2\ kHz}$)	-1.02	0.18	-5.7	<0.001		
Level (β_2)	0.1	0.008	13.1	<0.001	171 [1,365]	<0.001

Table 2. Summary of linear mixed-effects model and ANOVA with the dependent variable, MEM_{τ}, and predictors, frequency, level (77-95), df = degrees of freedom.

Mixed-effects model results					ANOVA	
Fixed effect	Estimates	Standard error	T-value	*p-value*	*F*-statistic [df]	*p*-value
Intercept ($\beta_{0\text{-}1kHz}$)	0.17	0.02	7.5	<0.001	1.12 [5,239]	0.34
Frequency ($\beta_{1\text{-}1.3\ kHz}$)	0.01	0.03	0.52	0.61		
Frequency ($\beta_{1\text{-}1.6\ kHz}$)	-0.01	0.03	-0.41	0.68		
Frequency ($\beta_{1\text{-}2\ kHz}$)	0.04	0.03	1.34	0.18		
Frequency ($\beta_{1\text{-}2.5\ kHz}$)	0.04	0.03	1.47	0.14		
Frequency ($\beta_{1\text{-}3.2\ kHz}$)	0.02	0.03	0.75	0.46		
Level (β_2)	0.001	0.001	1.6	0.1	2.56 [1,232]	0.11

Figure captions

Fig. 1. (color online) Top panels show one example of typical MEMR time course (left panel) and one example of atypical MEMR time course (right panel) from two different participants. In both top panels, colors indicate the third-octave band center frequency and scatter points are Δ at each time point in the time series (see Eq. 3). The line fits are double-exponential models fit to the data (see Eq. 4). Data are change in stimulus level re: the first time point (t_{16ms}). The difference between typical and atypical examples is that the change in Δ occurs in the unexpected direction. Although atypical, this behavior has previously been documented (for more details see section: *Idiosyncrasies in MEM time series likely reflect stapedius muscle behavior*). Data from the experiment run in an ear simulator is shown in the bottom panel. Only the 1 kHz band, but at all

stimulus levels, are shown for clarity. Notice that there is no evidence of MEMR activation.

Fig. 2. (color online) Group mean time series (panels by stimulus level). In each panel, colors represent the different third-octave frequency bands. Data are change in stimulus level re: the first time point (t_{16ms}). Only the fits to the group mean data are shown for easy visualization. The y-axis of the top panels has been zoomed in to examine smaller changes clearly. To maintain perspective, this zoomed region has been shaded with the same grey in the lower panels where the MEM is much larger. Three noteworthy aspects of these plots are (1) the MEM increases with increase in level and (2) different frequencies show different direction of change and (3) the MEM is different across frequencies. The magnitude and time-constants for each frequency are provided within panels.

Fig. 3. (color online) Box plots (panels by stimulus level) show individual MEM as filled circles on each box. Colors represent frequency in the x-axis. In the box plots, the white circle is the median and the thin vertical line is the data range. The horizontal, colored, line is the mean. A box plot is not plotted when there are no MEMR activations.

Fig. 4. (color online) Group mean time series (panels by frequency). Data are line fits to the change in stimulus level re: the first time point (t_{16ms}). In each panel growth in MEM with increasing level, i.e., level series, is plotted. Darker the shade of a given color, higher the stimulus level. As expected, the magnitude of the time series increases with increasing level. There is also a clear dichotomy in the direction of stimulus change as a function of frequency.

Fig. 5. (color online) Input/output functions of the MEM are plotted in the left 6 panels (panels by frequency). Thin colored lines are individual single exponential fits to the absolute MEM at each level in a given frequency. The thick colored line in each panel is the single exponential fit to the mean MEM at each frequency. For a better comparison of this growth across frequencies, only the fits to the group mean are plotted in the panel MEM-IO. The difference in growth across frequencies is striking, with the largest growth seen at 1 kHz and the smallest at 2 kHz. In the panel MEM-Tx, each line is a stimulus level with the MEM plotted as a function of frequency. This provides a transfer function of the MEM. Note the slight notch at 2 kHz, where the MEMR has the least influence.

Fig. 6. (color online) Box plots (panels by stimulus level), similar to Fig. 3., but show individual MEM_{τ} as filled circles in each box (see Fig. 3 caption for details on box plots). Unlike the MEM there is not clear pattern in MEM_{τ} as a function of level or frequency.

Fig. 7. (color online) Percentage of MEMR detections, i.e., %detections as a function of frequency, at each level (separated by panels) is presented as bar graphs in the left 6 panels. In the Fits panel, these detections are fit with a logistic function with colors representing frequencies. Dashed lines around the steepest and the shallowest fits are included to show the margin of error of the fits. The horizontal dashed grey line

indicates 95% detection. The vertical lines bookend the lowest and highest level, across frequencies, at which the 95% of the participants have MEMR activation.

Fig. 8. Scatter plot of MEMR thresholds obtained in the present study vs. those obtained for the same participants in a clinical tympanometer. The diagonal line shows unity relationship between the two variables. Notice that all but one data point fall above the unity line suggesting that the MEMR thresholds obtained in a clinical tympanometer were higher than that estimated by the current method.

References

Abdala, C., Mishra, S., & Garinis, A. (2013). Maturation of the human medial efferent reflex revisited. *The Journal of the Acoustical Society of America*, *133*(2), 938–950. http://doi.org/10.1121/1.4773265

Backus, B. C., & Guinan, J. J. (2006). Time-course of the human medial olivocochlear reflex. *The Journal of the Acoustical Society of America*, *119*(5), 2889–2904. http://doi.org/10.1121/1.2169918

Backus, B. C., & Guinan, J. J. (2007). Measurement of the Distribution of Medial Olivocochlear Acoustic Reflex Strengths Across Normal-Hearing Individuals via Otoacoustic Emissions. *Journal of the Association for Research in Otolaryngology*, *8*(4), 484–496. http://doi.org/10.1007/s10162-007-0100-0

Bates, D., Mächler, M., Bolker, B., & Walker, S. (2015). Fitting Linear Mixed-Effects Models Using lme4. *Journal of Statistical Software*, *67*(1). http://doi.org/10.18637/jss.v067.i01

Benjamini, Y., & Hochberg, Y. (1995). Controlling the False Discovery Rate - a Practical and Powerful Approach to Multiple Testing. *Journal of the Royal Statistical Society Series B-Methodological*, *57*, 289–300.

Bennett, M. J., & Weatherby, L. A. (1979). Multiple probe frequency acoustic reflex measurements. *Scandinavian Audiology*, *8*(4), 233–239. http://doi.org/10.3109/01050397909076325

Boothalingam, S., & Purcell, D. W. (2015). Influence of the stimulus presentation rate on medial olivocochlear system assays. *The Journal of the Acoustical Society of America*, *137*(2), 724–732. http://doi.org/10.1121/1.4906250

Borg, E. (1968). A Quantitative Study of the Effect of the Acoustic Stapedius Reflex on Sound transmission Through the Middle Ear of Man. *Acta Oto-Laryngologica*, *66*(1-6), 461–472. http://doi.org/10.3109/00016486809126311

Brown, M. C. (2014). Single-unit labeling of medial olivocochlear neurons: the cochlear frequency map for efferent axons. *Journal of Neurophysiology*, *111*(11), 2177–2186. http://doi.org/10.1152/jn.00045.2014

Cooper, N. P., & Yates, G. K. (1994). Nonlinear input-output functions derived from the responses of guinea-pig cochlear nerve fibres: Variations with characteristic frequency. *Hearing Research*, *78*(2), 221–234. http://doi.org/10.1016/0378-5955(94)90028-0

Dallos, P. J. (1964). Dynamics of the Acoustic Reflex: Phenomenological Aspects. *The Journal of the Acoustical Society of America*, *36*(11), 2175–2183. http://doi.org/10.1121/1.1919340

Dewey, J. B., & Dhar, S. (2017). Profiles of Stimulus-Frequency Otoacoustic Emissions from 0.5 to 20 kHz in Humans. *Journal of the Association for Research in Otolaryngology*, *18*(1), 89–110. http://doi.org/10.1007/s10162-016-0588-2

Feeney, M. P., & Keefe, D. H. (2001). Estimating the acoustic reflex threshold from wideband measures of reflectance, admittance, and power. *Ear and Hearing*, *22*(4), 316–332. http://doi.org/10.1097/00003446-200108000-00006

Feeney, M. P., Keefe, D. H., & Marryott, L. P. (2003). Contralateral acoustic reflex thresholds for tonal activators using wideband energy reflectance and admittance. *Journal of Speech, Language, and Hearing Research*, *46*(1), 128–136.

Feeney, M. P., Keefe, D. H., Hunter, L. L., Fitzpatrick, D. F., Garinis, A. C., Putterman, D. B., & McMillan, G. P. (2017). Normative Wideband Reflectance, Equivalent Admittance at the Tympanic Membrane, and Acoustic Stapedius Reflex Threshold in Adults. *Ear and Hearing*, *38*(3), e142–e160. http://doi.org/10.1097/AUD.0000000000000399

Gelfand, S. A. (2004). Hearing: An Introduction to Psychological and Physiological Acoustics (4 ed.). New York: Marcel Decker.

Goodman, S. S. (2017). Auditory Research Lab audio software. Iowa City : GitHub. Retrieved from https://github.com/myKungFu/ARLas

Goodman, S. S., & Keefe, D. H. (2006). Simultaneous measurement of noise-activated middle-ear muscle reflex and stimulus frequency otoacoustic emissions. *Journal of the Association for Research in Otolaryngology*, *7*(2), 125–139. http://doi.org/10.1007/s10162-006-0028-9

Goodman, S. S., Fitzpatrick, D. F., Ellison, J. C., Jesteadt, W., & Keefe, D. H. (2009). High-frequency click-evoked otoacoustic emissions and behavioral thresholds in humans. *The Journal of the Acoustical Society of America*, *125*(2), 1014–1032. http://doi.org/10.1121/1.3056566

Goodman, S. S., Lee, C., Guinan, J. J., Jr, & Lichtenhan, J. T. (2020). The Spatial Origins of Cochlear Amplification assessed by Stimulus Frequency Otoacoustic Emissions. *Biophysical Journal*. https://doi.org/10.1016/j.bpj.2019.12.031

Goodman, S. S., Mertes, I. B., Lewis, J. D., & Weissbeck, D. K. (2013). Medial Olivocochlear-Induced Transient-Evoked Otoacoustic Emission Amplitude Shifts in Individual Subjects. *Journal of the Association for Research in Otolaryngology*, *14*(6), 829–842. http://doi.org/10.1007/s10162-013-0409-9

Goodman, S. S., Venkitakrishnan, S., Adkins, W. J., & Mueldener, L. D. (2018). Effects of middle-ear and medial olivocochlear reflexes on TEOAE frequency, magnitude, and phase. *AIP Conference Proceedings*, *1965*(1), 170004. http://doi.org/10.1063/1.5038537

Guinan, J. J. (2006). Olivocochlear efferents: anatomy, physiology, function, and the measurement of efferent effects in humans. *Ear and Hearing*, *27*(6), 589–607. http://doi.org/10.1097/01.aud.0000240507.83072.e7

Guinan, J. J., Backus, B. C., Lilaonitkul, W., & Aharonson, V. (2003). Medial Olivocochlear Efferent Reflex in Humans: Otoacoustic Emission (OAE) Measurement Issues and the Advantages of Stimulus Frequency OAEs. *Journal of the Association for Research in Otolaryngology*, *4*(4), 521–540. http://doi.org/10.1007/s10162-002-3037-3

Guinan, J. J., Joseph, M. P., & Norris, B. E. (1989). Brainstem facial-motor pathways from two distinct groups of stapedius motoneurons in the cat. *The Journal of Comparative Neurology*, *287*(1), 134–144. http://doi.org/10.1002/cne.902870110

Heller, R., Heller, Y., & Gorfine, M. (2013). A consistent multivariate test of association based on ranks of distances. *Biometrika*, *100*(2), 503–510.

Hung, I. J., & Dallos, P. (1972). Study of the acoustic reflex in human beings. I. Dynamic characteristics. *The Journal of the Acoustical Society of America*, *52*(4), 1168–1180. http://doi.org/10.1121/1.1913229

James, A. L., Harrison, R. V., Pienkowski, M., Dajani, H. R., & Mount, R. J. (2005). Dynamics of real time DPOAE contralateral suppression in chinchillas and humans. *International Journal of Audiology*, *44*(2), 118–129.

Jerger, J., & Hayes, D. (1983). Latency of the acoustic reflex in eighth-nerve tumor. *Arch Otolaryngol*, *109*(1), 1–5. http://doi.org/10.1001/archotol.1983.00800150005001

Keefe, D. H., Bulen, J. C., Arehart, K. H., & Burns, E. M. (1993). Ear-canal impedance and reflection coefficient in human infants and adults. *The Journal of the Acoustical Society of America*, *94*(5), 2617–2638. http://doi.org/10.1121/1.407347

Keefe, D. H., Fitzpatrick, D., Liu, Y.-W., Sanford, C. A., & Gorga, M. P. (2010). Wideband acoustic-reflex test in a test battery to predict middle-ear dysfunction. *Hearing Research*, *263*(1-2), 52–65.

Kim, D. O., Dorn, P. A., Neely, S. T., & Gorga, M. P. (2001). Adaptation of distortion product otoacoustic emission in humans. *Journal of the Association for Research in Otolaryngology*, *2*(1), 31–40.

Kobler, J. B., Guinan, J. J., Vacher, S. R., & Norris, B. E. (1992). Acoustic reflex frequency selectivity in single stapedius motoneurons of the cat. *Journal of Neurophysiology*, *68*(3), 807–817. http://doi.org/10.1152/jn.1992.68.3.807

Lee, D. J., de Venecia, R. K., Guinan, J. J., & Brown, M. C. (2006). Central auditory pathways mediating the rat middle ear muscle reflexes. *Anatomical Record Part a-Discoveries in Molecular Cellular and Evolutionary Biology*, *288*(4), 358–369. http://doi.org/10.1002/ar.a.20296

Lewis, J. D., & Goodman, S. S. (2014). Basal Contributions to Short-Latency Transient-Evoked Otoacoustic Emission Components. *Journal of the Association for Research in Otolaryngology*. http://doi.org/10.1007/s10162-014-0493-5

Liberman, M. C. (1978). Auditory-nerve response from cats raised in a low-noise chamber. *The Journal of the Acoustical Society of America*, *63*(2), 442–455. http://doi.org/10.1121/1.381736

Liberman, M. C., & Guinan, J. J. (1998). Feedback control of the auditory periphery: Anti-masking effects of middle ear muscles vs. olivocochlear efferents. *Journal of Communication Disorders*, *31*(6), 471–483. http://doi.org/10.1016/S0021-9924(98)00019-7

Liberman, M. C., Puria, S., & Guinan, J. J., Jr. (1996). The ipsilaterally evoked olivocochlear reflex causes rapid adaptation of the 2 f1− f2 distortion product otoacoustic emission. *The Journal of the Acoustical Society of America*, *99*(6), 3572–3584.

Lutman, M. E., & Martin, A. M. (1978). Adaptation of the acoustic reflex to combinations of sustained steady-state and repeated pulse stimuli. *Journal of Sound and Vibration Research*, *56*(1), 137–150.

Lutolf, J. J., O'Malley, H., & Silman, S. (2003). The effects of probe-tone frequency on the acoustic-reflex growth function. *Journal of the American Academy of Audiology*, *14*(2), 109–118. http://doi.org/10.3766/jaaa.14.2.6

Margolis, R. H., & Levine, S. C. (1991). Acoustic reflex measures in audiologic evaluation. *Otolaryngologic Clinics of North America*, *24*(2), 329–347.

Marks, K. L., & Siegel, J. H. (2017). Differentiating Middle Ear and Medial Olivocochlear Effects on Transient-Evoked Otoacoustic Emissions. *Journal of the Association for Research in Otolaryngology*, *121*, 1588–14. http://doi.org/10.1007/s10162-017-0621-0

Marshall, L., Lapsley Miller, J. A., Guinan, J. J., Shera, C. A., Reed, C. M., Perez, Z. D., et al. (2014). Otoacoustic-emission-based medial-olivocochlear reflex assays for humans. *The Journal of the Acoustical Society of America*, *136*(5), 2697. http://doi.org/10.1121/1.4896745

Meinke, D. K., Stagner, B. B., Martin, G. K., & Lonsbury-Martin, B. L. (2005). Human efferent adaptation of DPOAEs in the L1,L2 space. *Hearing Research*, *208*(1-2), 89–100. http://doi.org/10.1016/j.heares.2005.05.004

Mertes, I. B. (2020). Medial olivocochlear reflex effects on synchronized spontaneous otoacoustic emissions. *The Journal of the Acoustical Society of America*, *147*(3), EL235–EL240. http://doi.org/10.1121/10.0000886

Mertes, I. B., & Goodman, S. S. (2015). Within-and Across-Subject Variability of Repeated Measurements of Medial Olivocochlear-Induced Changes in Transient-Evoked Otoacoustic Emissions. *Ear and Hearing*.

Mukerji, S., Windsor, A. M., & Lee, D. J. (2010). Auditory Brainstem Circuits That Mediate the Middle Ear Muscle Reflex. *Trends in Amplification*, *14*(3), 170–191. http://doi.org/10.1177/1084713810381771

Neergaard, E. B., & Rasmussen, P. E. (1966). Latency of the stapedius muscle reflex in man. *Arch Otolaryngol*, *84*(2), 173–180.

Perlman, H. B., & Case, T. J. (1939). Latent Period of the Crossed Stapedius Reflex in Man. *Annals of Otology, Rhinology & Laryngology*, *48*(3), 663–675. http://doi.org/10.1177/000348943904800311

Popelka, G. R., Karlovich, R. S., & Wiley, T. L. (1974). Acoustic reflex and critical bandwidth. *The Journal of the Acoustical Society of America*, *55*(4), 883–885. http://doi.org/10.1121/1.1914619

R Core Team. R: A language and environment for statistical computing (v3.6.0). Vienna, Austria: R Foundation for Statistical Computing.

Rabinowitz, W. M. (1977). *Acoustic-reflex effects on the input admittance and transfer characteristics of the human middle-ear.* Unpublished PhD Thesis: Massachusetts Institute of Technology, Boston.

Scheperle, R. A., Neely, S. T., Kopun, J. G., & Gorga, M. P. (2008). Influence of in situ, sound-level calibration on distortion-product otoacoustic emission variability. *The Journal of the Acoustical Society of America*, *124*(1), 288. http://doi.org/10.1121/1.2931953

Rasetshwane, D. M., & Neely, S. T. (2011). Inverse solution of ear-canal area function from reflectance. *The Journal of the Acoustical Society of America*, *130*(6), 3873–3881. http://doi.org/10.1121/1.3654019

Robles, L., & Ruggero, M. A. (2001). Mechanics of the mammalian cochlea. *Physiological Reviews*, *81*(3), 1305–1352.

Shera, C. A., Guinan, J. J., & Oxenham, A. J. (2002). Revised estimates of human cochlear tuning from otoacoustic and behavioral measurements. *Proceedings of the National Academy of Sciences of the United States of America*, *99*(5), 3318–3323. http://doi.org/10.1073/pnas.032675099

Souza, N. N., Dhar, S., Neely, S. T., & Siegel, J. H. (2014). Comparison of nine methods to estimate ear-canal stimulus levels. *The Journal of the Acoustical Society of America*, *136*(4), 1768–1787. http://doi.org/10.1121/1.4894787

Sprague, B. H., Wiley, T. L., & Block, M. G. (1981). Dynamics of acoustic reflex growth. *Audiology*, *20*(1), 15–40.

Srinivasan, S., Keil, A., Stratis, K., Woodruff Carr, K. L., & Smith, D. W. (2012). Effects of cross-modal selective attention on the sensory periphery: Cochlear sensitivity is altered by selective attention. *Neuroscience*, *223*, 325–332. http://doi.org/10.1016/j.neuroscience.2012.07.062

Stach, B. A. (1987). The acoustic reflex in diagnostic audiology: from Metz to present. *Ear and Hearing*, *8*(4 Suppl), 36S–42S. http://doi.org/10.1097/00003446-198708001-00008

Valero, M. D., Hancock, K. E., Maison, S. F., & Liberman, M. C. (2018). Effects of cochlear synaptopathy on middle-ear muscle reflexes in unanesthetized mice. *Hearing Research*. http://doi.org/10.1016/j.heares.2018.03.012

Wilson, R. H., Shanks, J. E., & Lily, D. J. (1984). Acoustic-Reflex Adaptation. In S. Silman (Ed.), *The Acoustic Reflex Basic Principles and Clinical Applications* (pp. 329–387). Orlando, Florida.

Wilson, R. H., Steckler, J. F., Jones, H. C., & Margolis, R. H. (1978). Adaptation of the acoustic reflex. *The Journal of the Acoustical Society of America*, *64*(3), 782–791. http://doi.org/10.1121/1.382043

Zhao, W., & Dhar, S. (2009). The Effect of Contralateral Acoustic Stimulation on Spontaneous Otoacoustic Emissions. *Journal of the Association for Research in Otolaryngology*, *11*(1), 53–67. http://doi.org/10.1007/s10162-009-0189-4

Fig 1

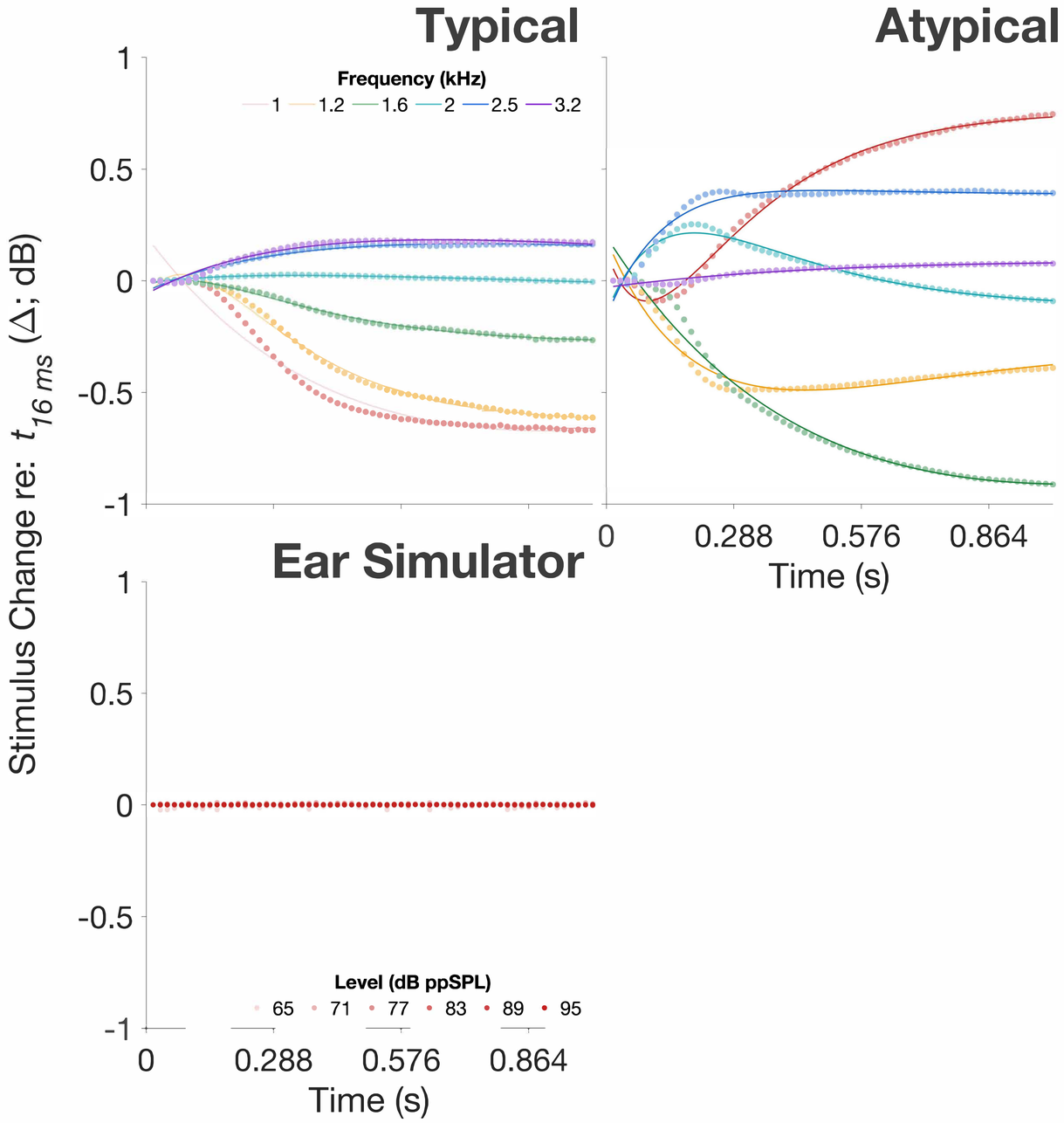
Typical
Atypical
Ear Simulator
Frequency (kHz)
1
1.2
1.6
2
2.5
3.2
Level (dB ppSPL)
65
71
77
83
89
95
Stimulus Change re: $t_{16\ ms}$ (Δ; dB)
1
0.5
0
-0.5
-1
0
0.288
0.576
0.864
Time (s)

Fig 2

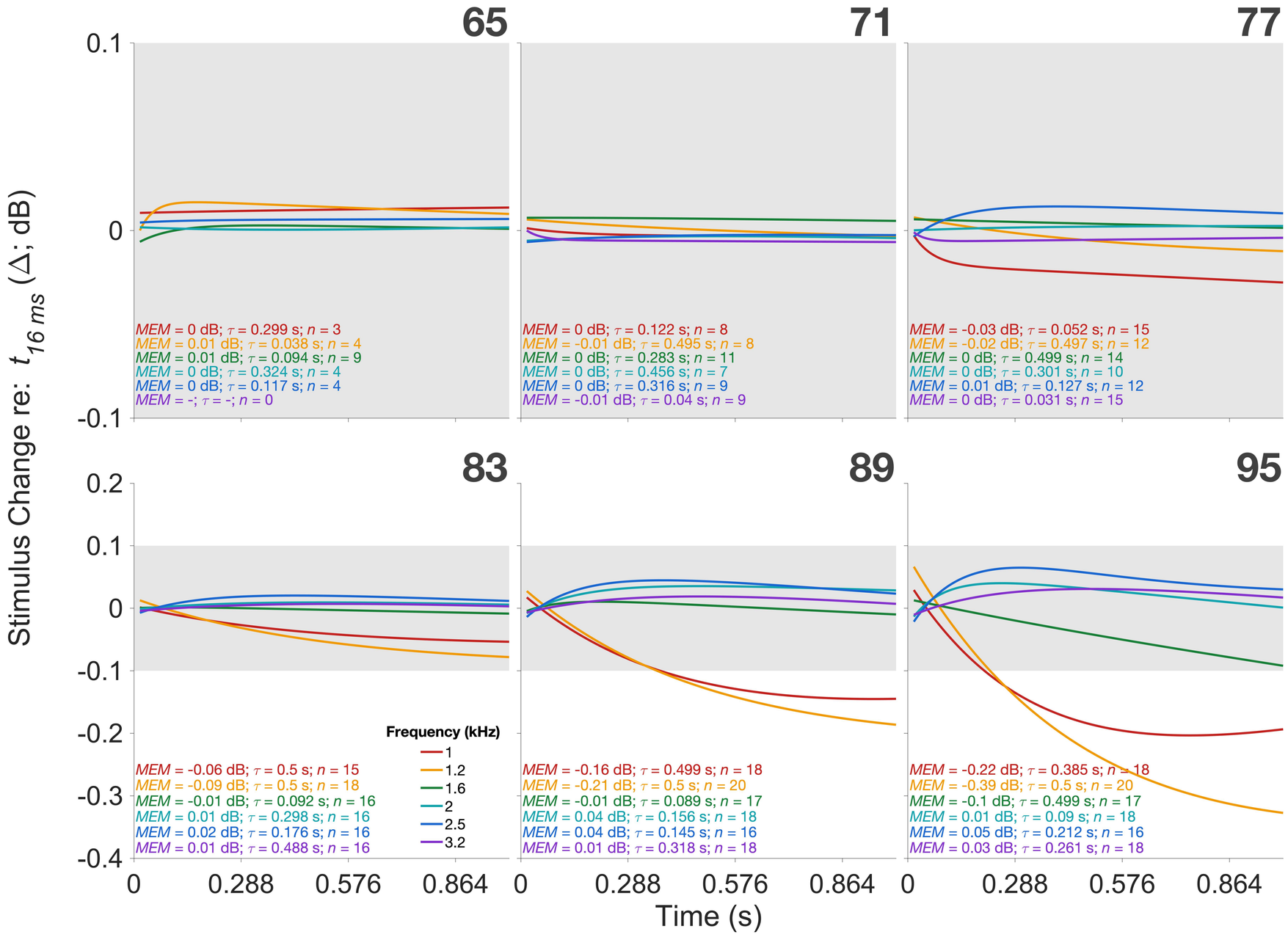
65
71
77
83
89
95
Stimulus Change re: $t_{16\ ms}$ (Δ; dB)
Time (s)
0.1
0
-0.1
0.2
-0.2
-0.3
-0.4
0
0.288
0.576
0.864
MEM = 0 dB; τ = 0.299 s; n = 3
MEM = 0.01 dB; τ = 0.038 s; n = 4
MEM = 0.01 dB; τ = 0.094 s; n = 9
MEM = 0 dB; τ = 0.324 s; n = 4
MEM = 0 dB; τ = 0.117 s; n = 4
MEM = -; τ = -; n = 0
MEM = 0 dB; τ = 0.122 s; n = 8
MEM = -0.01 dB; τ = 0.495 s; n = 8
MEM = 0 dB; τ = 0.283 s; n = 11
MEM = 0 dB; τ = 0.456 s; n = 7
MEM = 0 dB; τ = 0.316 s; n = 9
MEM = -0.01 dB; τ = 0.04 s; n = 9
MEM = -0.03 dB; τ = 0.052 s; n = 15
MEM = -0.02 dB; τ = 0.497 s; n = 12
MEM = 0 dB; τ = 0.499 s; n = 14
MEM = 0 dB; τ = 0.301 s; n = 10
MEM = 0.01 dB; τ = 0.127 s; n = 12
MEM = 0 dB; τ = 0.031 s; n = 15
Frequency (kHz)
1
1.2
1.6
2
2.5
3.2
MEM = -0.06 dB; τ = 0.5 s; n = 15
MEM = -0.09 dB; τ = 0.5 s; n = 18
MEM = -0.01 dB; τ = 0.092 s; n = 16
MEM = 0.01 dB; τ = 0.298 s; n = 16
MEM = 0.02 dB; τ = 0.176 s; n = 16
MEM = 0.01 dB; τ = 0.488 s; n = 16
MEM = -0.16 dB; τ = 0.499 s; n = 18
MEM = -0.21 dB; τ = 0.5 s; n = 20
MEM = -0.01 dB; τ = 0.089 s; n = 17
MEM = 0.04 dB; τ = 0.156 s; n = 18
MEM = 0.04 dB; τ = 0.145 s; n = 16
MEM = 0.01 dB; τ = 0.318 s; n = 18
MEM = -0.22 dB; τ = 0.385 s; n = 18
MEM = -0.39 dB; τ = 0.5 s; n = 20
MEM = -0.1 dB; τ = 0.499 s; n = 17
MEM = 0.01 dB; τ = 0.09 s; n = 18
MEM = 0.05 dB; τ = 0.212 s; n = 16
MEM = 0.03 dB; τ = 0.261 s; n = 18

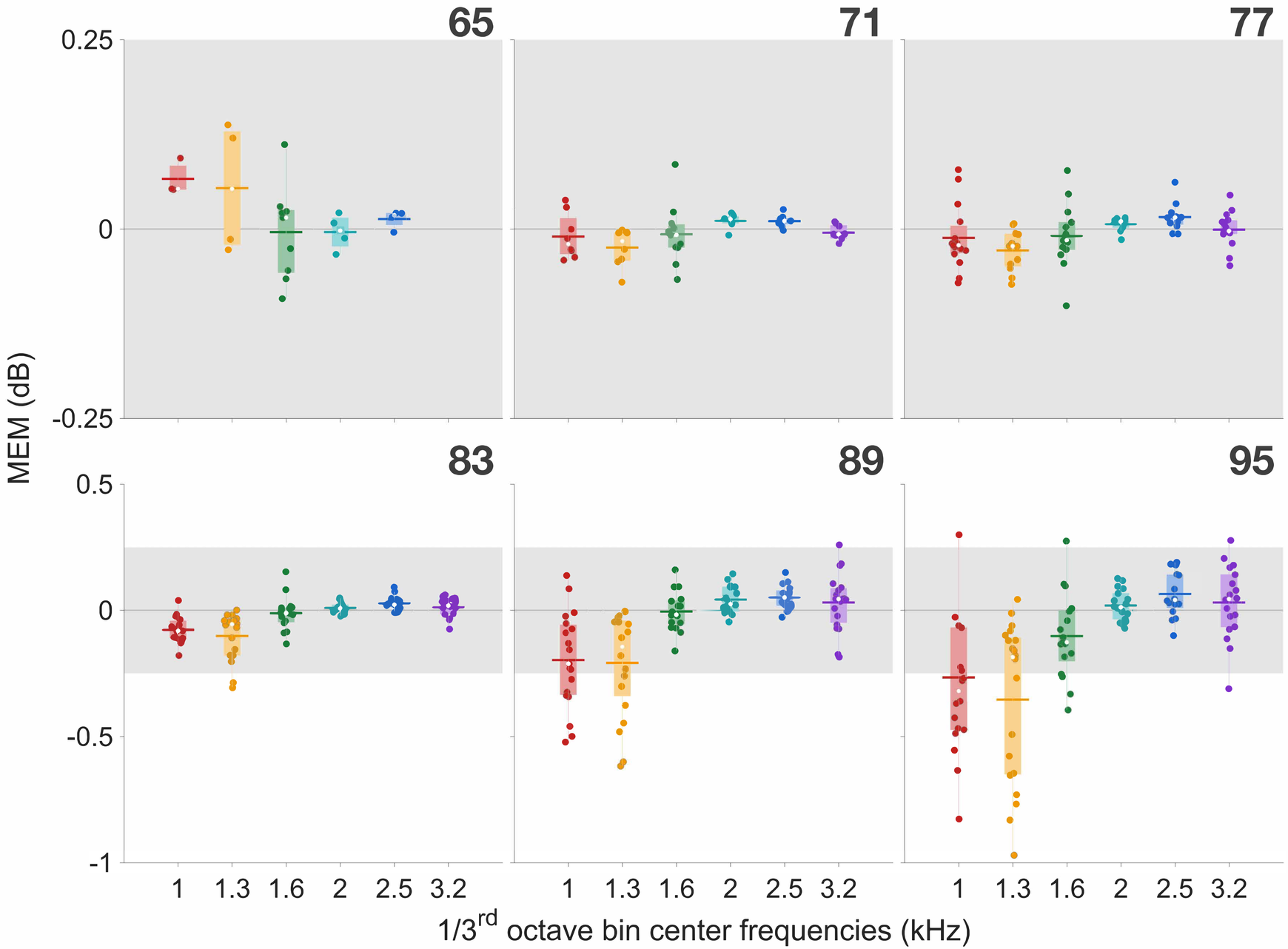
65
71
77
83
89
95
0.25
0
-0.25
0.5
0
-0.5
-1
MEM (dB)
1
1.3
1.6
2
2.5
3.2
1/3rd octave bin center frequencies (kHz)

Fig 3

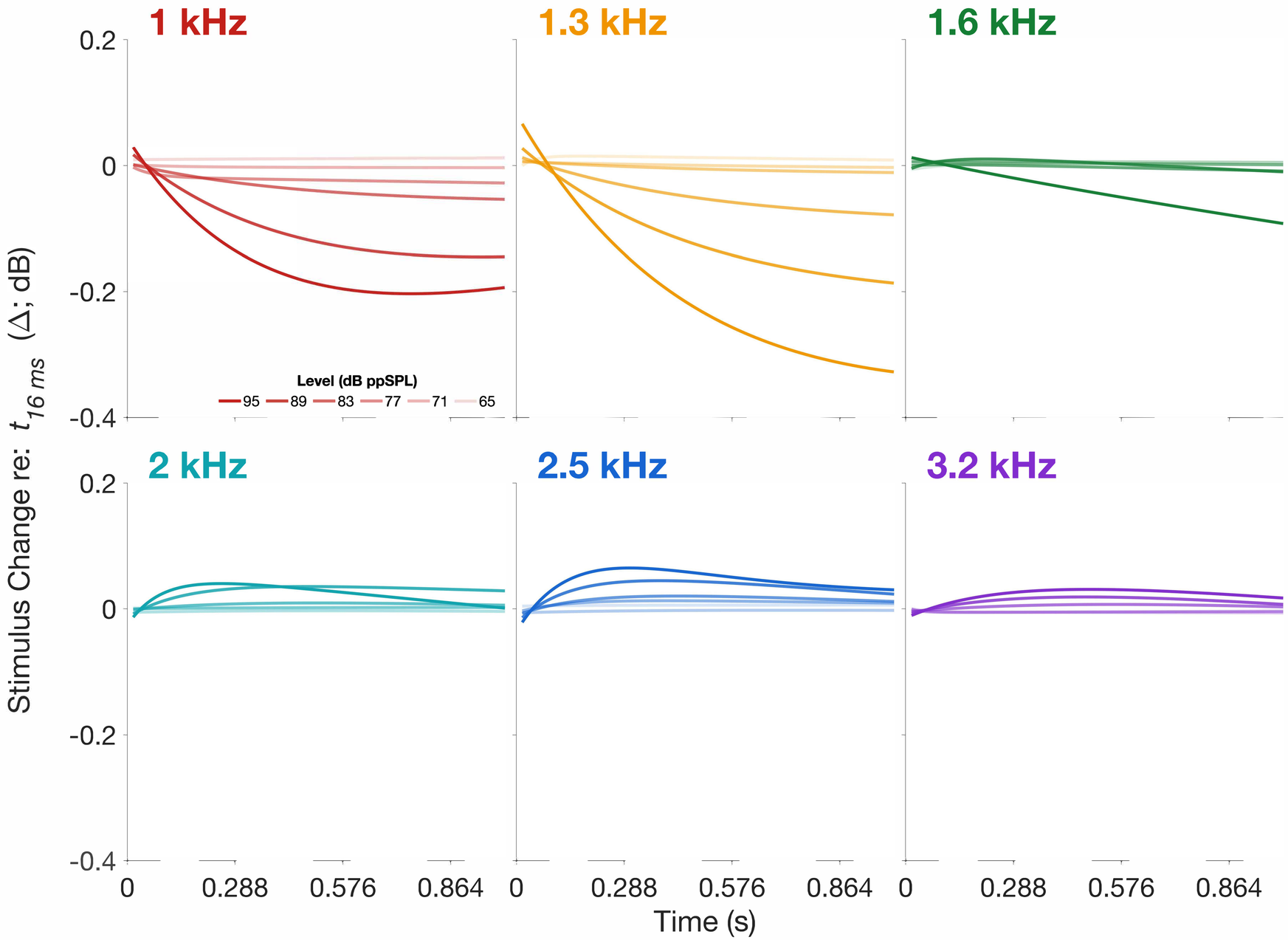
1 kHz
1.3 kHz
1.6 kHz
2 kHz
2.5 kHz
3.2 kHz
Level (dB ppSPL)
95
89
83
77
71
65
0.2
0
-0.2
-0.4
0
0.288
0.576
0.864
Time (s)
Stimulus Change re: $t_{16\ ms}$ (Δ; dB)

Fig 4

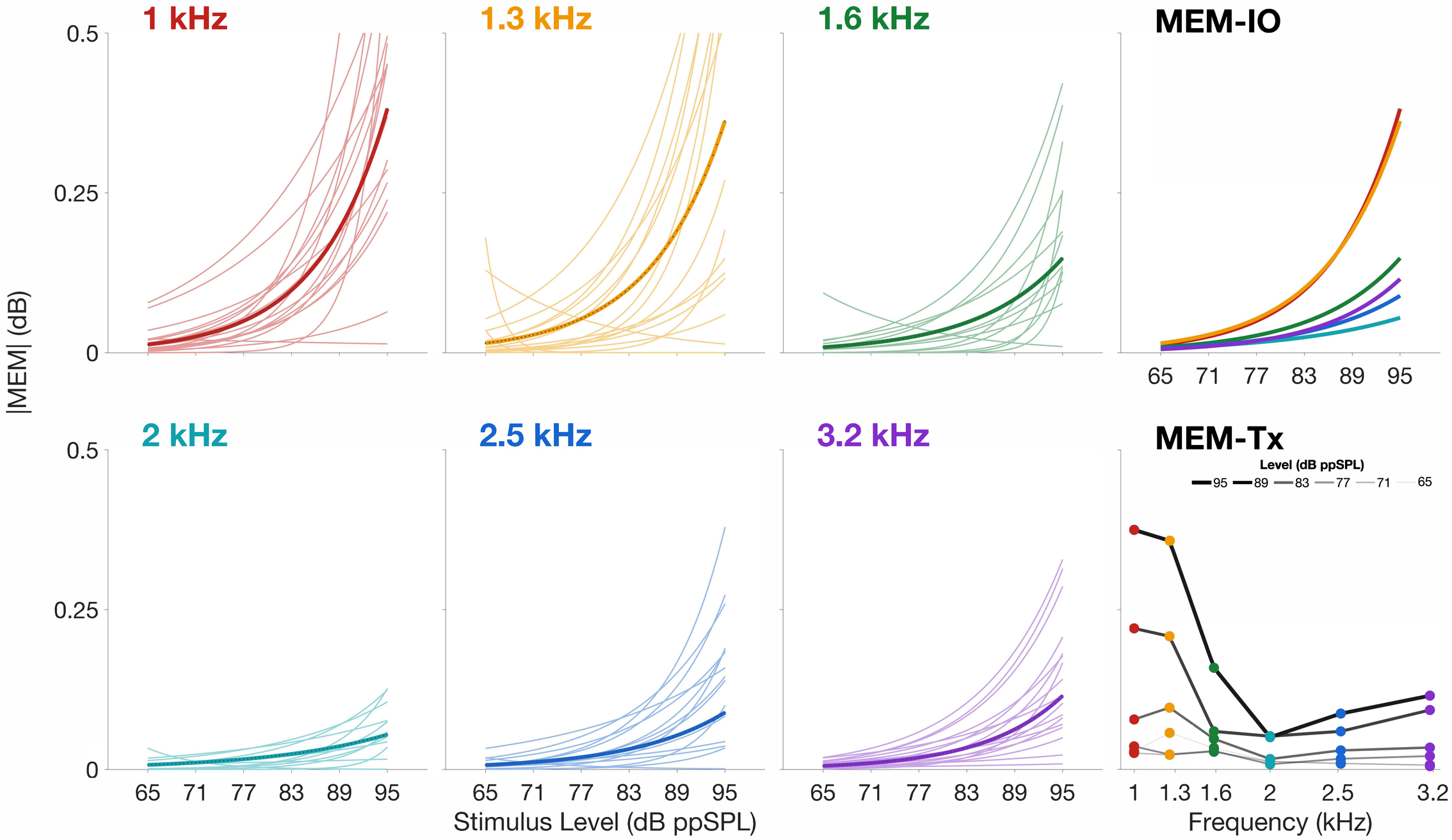
Fig 5
1 kHz
1.3 kHz
1.6 kHz
MEM-IO
2 kHz
2.5 kHz
3.2 kHz
MEM-Tx
|MEM| (dB)
0.5
0.25
0
65 71 77 83 89 95
Stimulus Level (dB ppSPL)
Level (dB ppSPL)
95 89 83 77 71 65
1 1.3 1.6 2 2.5 3.2
Frequency (kHz)

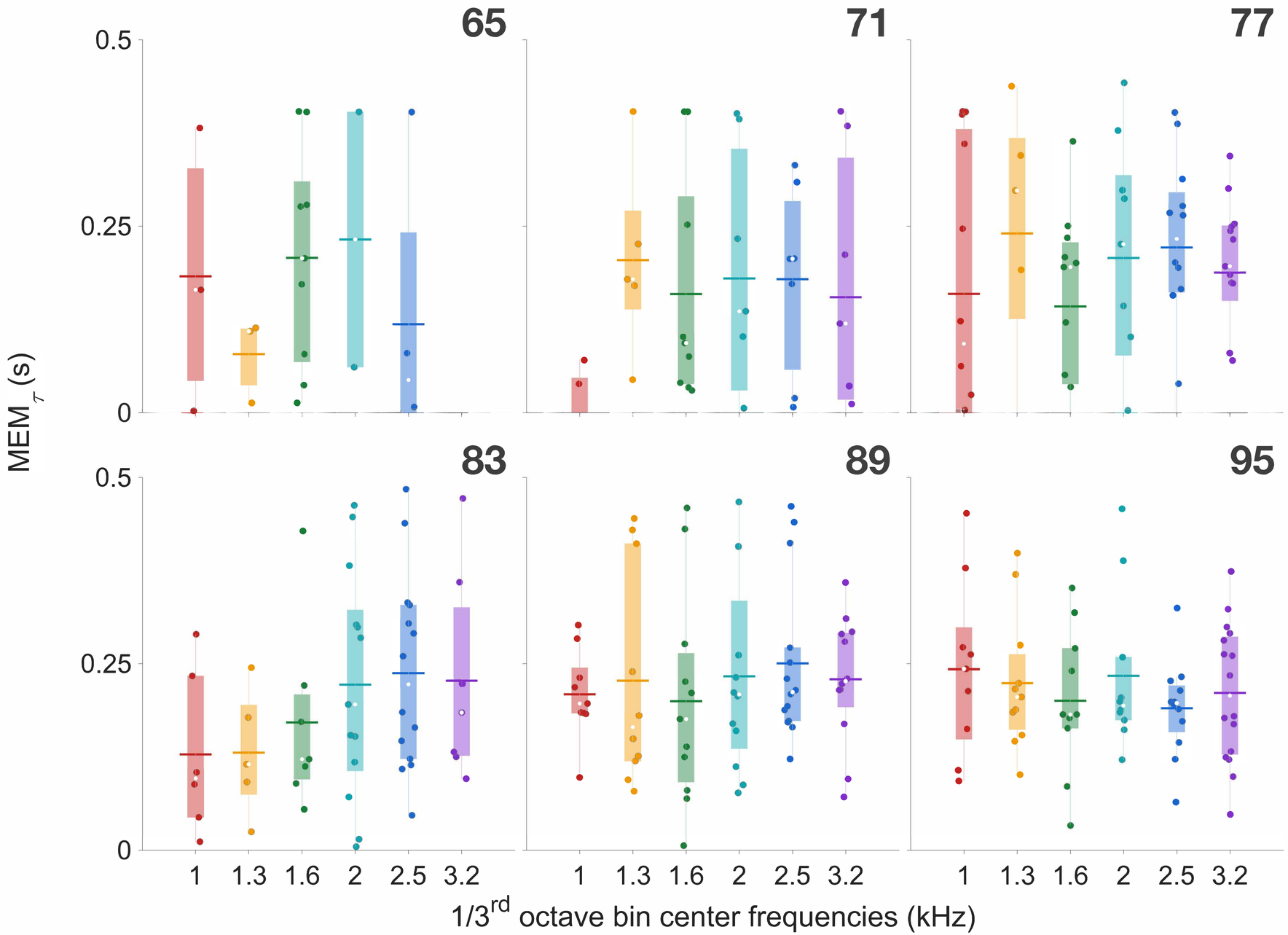
65
71
77
83
89
95
0.5
0.25
0
MEM$_\tau$ (s)
1
1.3
1.6
2
2.5
3.2
1/3rd octave bin center frequencies (kHz)

Fig 6

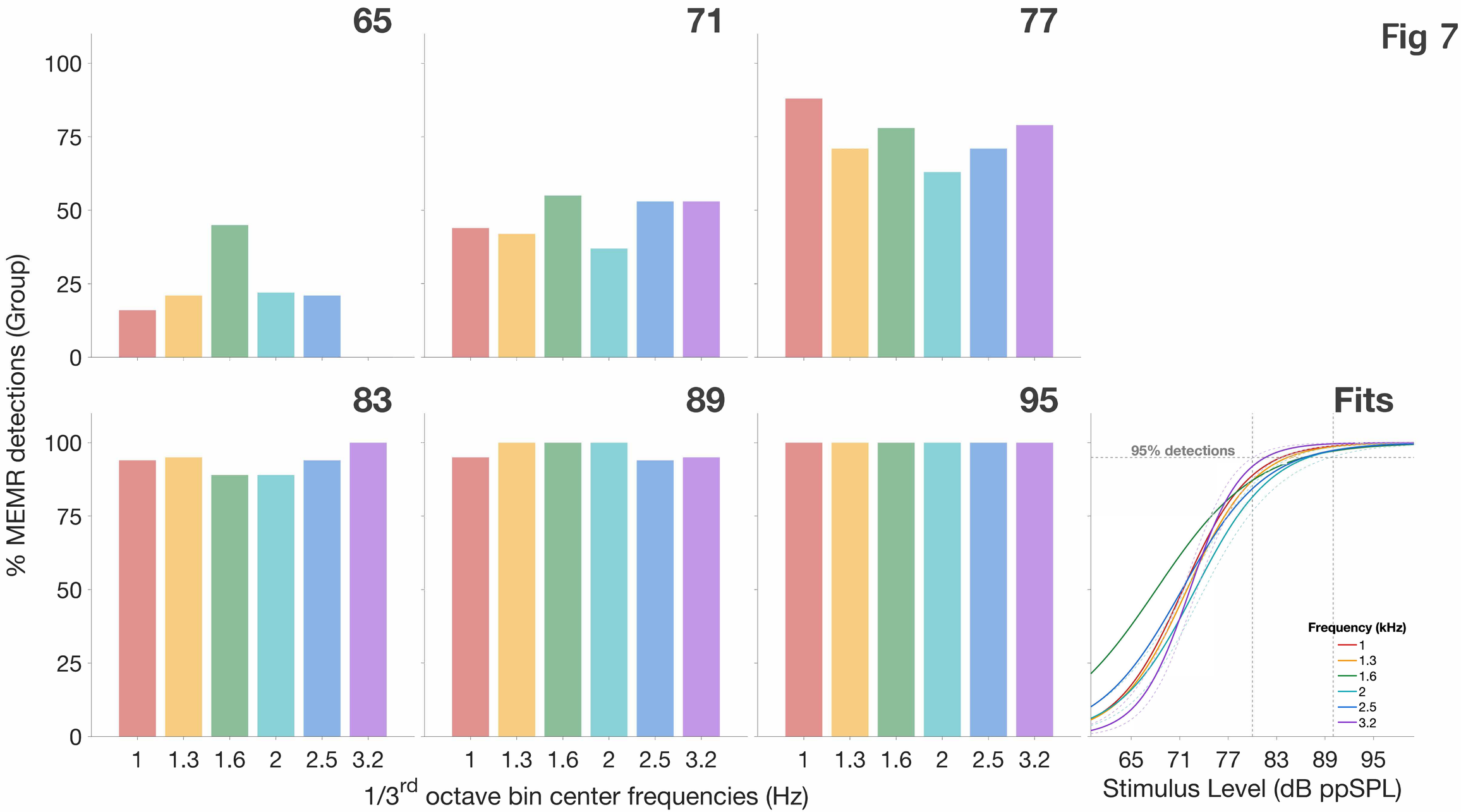
Fig 7
65
71
77
83
89
95
Fits
% MEMR detections (Group)
100
75
50
25
0
1
1.3
1.6
2
2.5
3.2
1/3rd octave bin center frequencies (Hz)
95% detections
Frequency (kHz)
1
1.3
1.6
2
2.5
3.2
65
71
77
83
89
95
Stimulus Level (dB ppSPL)

Fig 8

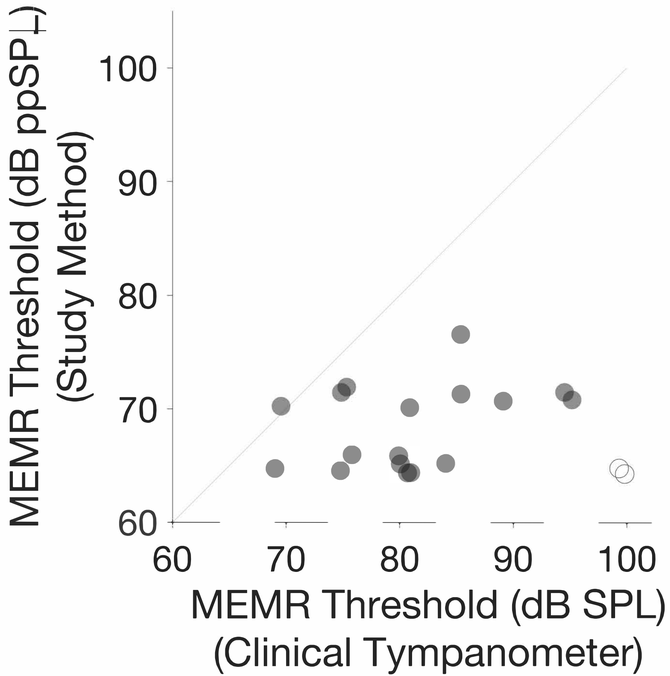
MEMR Threshold (dB ppSPL)
(Study Method)
100
90
80
70
60
60
70
80
90
100
MEMR Threshold (dB SPL)
(Clinical Tympanometer)